Adsorption 2, 133–143 (1996)

Analysis of ZLC Desorption Curves for Gaseous Systems

STEFANO BRANDANI* AND DOUGLAS M. RUTHVEN
Department of Chemical Engineering, University of Maine, Orono, ME 04469

Received December 15, 1994; Revised October 11, 1995; Accepted October 19, 1995

Abstract. The theoretical model and underlying assumptions used in the analysis of ZLC (zero length column) desorption curves are examined in detail. It is shown that the long time analysis generally yields reliable diffusivity values although, if the initial equilibrium condition is not properly established there will be significant error in the apparent equilibrium constant. The short time analysis is much more sensitive to such errors and a modified way of data analysis is suggested to overcome this problem. Varying the initial equilibration time provides an alternative ZLC experiment that can be used to establish the nature of the rate controlling mass transfer resistance. The utility of this approach is illustrated experimentally for the system C_3H_8-13X zeolite.

Keywords: diffusion, sorption kinetics, ZLC

The zero length column (ZLC) method of measuring intracrystalline (or intraparticle) diffusion depends on following the desorption of sorbate from a previously equilibrated (small) sample of adsorbent into an inert carrier stream. The technique is simple and relatively inexpensive and since its introduction in 1988 (Eic and Ruthven, 1988) it has been widely used to study both micropore and macropore diffusion (Ruthven and Eic, 1988; Voogd et al., 1991; Ruthven and Xu, 1993) as well as to follow exchange counter-diffusion in liquid phase adsorption (Ruthven and Stapleton, 1993) and tracer exchange in a vapour system (Hufton and Ruthven, 1993). In most of these studies the experimental desorption curves were interpreted according to the original simplified model of Eic and Ruthven (1988), although a more sophisticated numerical approach has recently been suggested (Micke, Kocirik, and Bulow, 1994). The simple model provides an adequate approximation over a wide range of conditions but there are certain practically important situations where a more accurate representation is required. Furthermore, the traditional analysis utilizes only the long time region of the desorption curve, where the measurement of the relative concentration is subject to the greatest experimental error. The initial portion of the desorption curve can be measured with greater accuracy and, although the possibility of using initial rate data was suggested by Hufton and Ruthven (1994), to establish the range and limitations of their approximate model requires a more detailed analysis. The analysis presented here makes it possible to establish the limitations of the earlier models and it has led also to the development of a modified experimental technique which can provide additional information. These developments of the theory and experimental technique are reported here.

The Traditional Model (Eic and Ruthven, 1988)

In the original development the adsorbent particles are assumed spherical with a linear equilibrium condition at the particle (crystal) surface. The governing equations are:

$$\frac{\partial q}{\partial t} = D\left(\frac{\partial^2 q}{\partial r^2} + \frac{2}{r}\frac{\partial q}{\partial r}\right) \qquad (1)$$

---

*Permanent address: Dipartimento di Chimica, Ingegneria Chimica e Materiali, Università de L'Aquila, I-67040 Monteluco di Roio, L'Aquila, Italy.

$$\frac{\partial q}{\partial r}(0,t) = 0; \quad q(R,t) = Kc(t);$$

$$q(r,0) = q_0 = Kc_0 \tag{2}$$

$$D\frac{\partial q}{\partial r}(R,t) + \frac{1}{3}\frac{FR}{V_s K}q(R,t) = 0 \tag{3}$$

Equation (3) is the boundary condition at the particle surface resulting from a mass balance over the cell. The basic assumptions are equilibrium at the particle surface, perfect mixing through the cell and neglect of hold-up in the fluid phase in comparison with the adsorbed phase hold-up. The solution is readily obtained by separation of variables or directly from known solutions (Crank, 1956).

The resulting expression for the desorption curve is:

$$\frac{c}{c_0} = 2L\sum_{n=1}^{\infty}\frac{\exp\left(-\frac{\beta_n^2 Dt}{R^2}\right)}{\left[\beta_n^2 + L(L-1)\right]} \tag{4}$$

where β_n is given by the roots of;

$$\beta_n \cot\beta_n + L - 1 = 0 \tag{5}$$

and

$$L = \frac{1}{3}\frac{FR^2}{KV_s D} \tag{6}$$

The corresponding expressions for a parallel sided adsorbent slab (half-thickness 1) are:

$$\frac{c}{c_0} = 2L\sum_{n=1}^{\infty}\frac{\exp\left(-\frac{\beta_n^2 Dt}{l^2}\right)}{\left[\beta_n^2 + L(L+1)\right]} \tag{7}$$

where β_n is given by:

$$\beta_n \tan\beta_n = L = \frac{Fl^2}{KV_s D} \tag{8}$$

In the long time region Eqs. (4) and (7) reduce to simple exponential decay curves since only the first term of the summation is significant:

$$\frac{c}{c_0} = \frac{2L}{\left[\beta_1^2 - L(L-1)\right]}\exp\left(-\frac{\beta_1^2 Dt}{R^2}\right) \tag{9}$$

with a corresponding expression for the parallel sided slab. A plot of in $\ln(c/c_0)$ vs. t should therefore yield a linear asymptote, in the long time region, from the slope and intercept of which the parameters D and L can be found. This is the so called long time (LT) analysis.

There are two obvious problems with this model; hold-up in the fluid phase is neglected and the analysis (based on Eq. (9)) uses only the data from the tail of the desorption curve, which is the region of greatest experimental uncertainty. We have recently addressed the first of these problems by extending the model to include extracrystalline hold-up (Brandani and Ruthven, 1995). The resulting expression for the desorption curve is

$$\frac{c}{c_0} = 2L\sum_{n=1}^{\infty}\frac{\exp\left(-\frac{\beta_n^2 Dt}{R^2}\right)}{\left[\beta_n^2 + \left(L - 1 - \gamma\beta_n^2\right) + L - 1 + \gamma\beta_n^2\right]} \tag{10}$$

where β_n are the positive roots of:

$$\beta_n \cot\beta_n + L - 1 - \gamma\beta_n^2 = 0 \tag{11}$$

in which $\gamma (= V_f/3KV_s)$ represents one third of the ratio of the external to internal hold-up. Clearly for $\gamma \rightarrow 0$ Eqs. (10) and (11) revert to Eqs. (4) and (5).

Comparison of the full and approximate solutions shows that, for $\gamma < 0.1$ there is little difference. This condition is almost always fulfilled for vapour phase systems but it is generally violated for liquid systems. One may therefore conclude that, for vapour systems, the neglect of external hold-up, as in the original simplified model, is generally a valid approximation and the validity of this approximation is assumed for the remainder of this paper.

Short Time Analysis

The initial portion of the desorption curve is less sensitive to the errors that may arise from baseline drift or from a finite rate of heat dissipation so, rather than relying entirely on the tail of the desorption curve it would be desirable to extract the kinetic parameters also from the initial region. A comparison between the short time (ST) and long time (LT) values could then be used as a check on the validity of the data.

The following Laplace domain solution to Eqs. (1–3) is readily derived:

$$\frac{\tilde{q}(r,s)}{q_0} = \frac{LR}{sr} \times \frac{\exp\left(-\sqrt{\frac{s}{D}}(R+r)\right) - \exp\left(-\sqrt{\frac{s}{D}}(R-r)\right)}{\exp\left(-2\sqrt{\frac{s}{D}}R\right)\left(\sqrt{\frac{s}{D}}R - L + 1\right) + \left(\sqrt{\frac{s}{D}}R + L - 1\right)} + \frac{1}{s} \tag{12}$$

from which the concentration at the particle surface

($r = R$) is obtained:

$$\frac{\tilde{c}}{c_0} = \frac{1}{s}\left[\frac{\sqrt{\frac{s}{D}}R\cosh\left(\sqrt{\frac{s}{D}}R\right) - \sinh\left(\sqrt{\frac{s}{D}}R\right)}{\sqrt{\frac{s}{D}}R\cosh\left(\sqrt{\frac{s}{D}}R\right) + (L-1)\sinh\left(\sqrt{\frac{s}{D}}R\right)}\right] \tag{13}$$

A general inversion of Eq. (13) to obtain the time domain solution ($c(t)$) is difficult. However, for the special case $L = 1$ the inversion is straightforward (Roberts and Kaufman, 1966) and yields:

$$\frac{c}{c_0} = 1 - 2\sqrt{\frac{D}{\pi R^2}} \times \left[\sqrt{t} - \sum_{n=1}^{\infty}\left((-1)^n \int_0^t \exp\frac{\left(-\frac{n^2R^2}{Du}\right)}{\sqrt{u}}du\right)\right] \tag{14}$$

In the short time region the terms within the summation are negligible so the initial portion of the desorption curve (for $L = 1$) can be represented simply by:

$$\frac{c}{c_0} = 1 - 2\sqrt{\frac{Dt}{\pi R^2}} \tag{15}$$

Figure 1 shows a family of theoretical desorption curves, calculated for various values of L from Eq. (7). It is evident that for $L = 1$ Eq. (15) is a valid approximation up to about 60% approach to equilibrium ($c/c_0 > 0.4$). To obtain the equivalent short time expression for the general case we consider the series expansion of the general solution Eq. (13):

$$\frac{\tilde{c}}{c_0} = \frac{1}{s}\left[\left(1 - \sqrt{\frac{D}{R^2 s}}\tanh\left(\sqrt{\frac{s}{D}}R\right)\right) \times \sum_{n=0}^{\infty}\left(-(L-1)\sqrt{\frac{D}{R^2 s}}\tanh\left(\sqrt{\frac{s}{D}}R\right)\right)^n\right] \tag{16}$$

from which, by considering only the first two terms ($n = 0, n = 1$) we obtain:

$$\frac{\tilde{c}}{c_0} = \frac{1}{s}\left[1 - L\sqrt{\frac{D}{sR^2}}\tanh\left(\sqrt{\frac{s}{D}}R\right)\right] - (L-1)\frac{D}{s^2R^2}\tanh^2\left(\sqrt{\frac{s}{D}}R\right) \tag{17}$$

which may be inverted directly to yield; for the short time solution:

$$\frac{c}{c_0} = 1 - 2L\sqrt{\frac{Dt}{\pi R^2}} \tag{18}$$

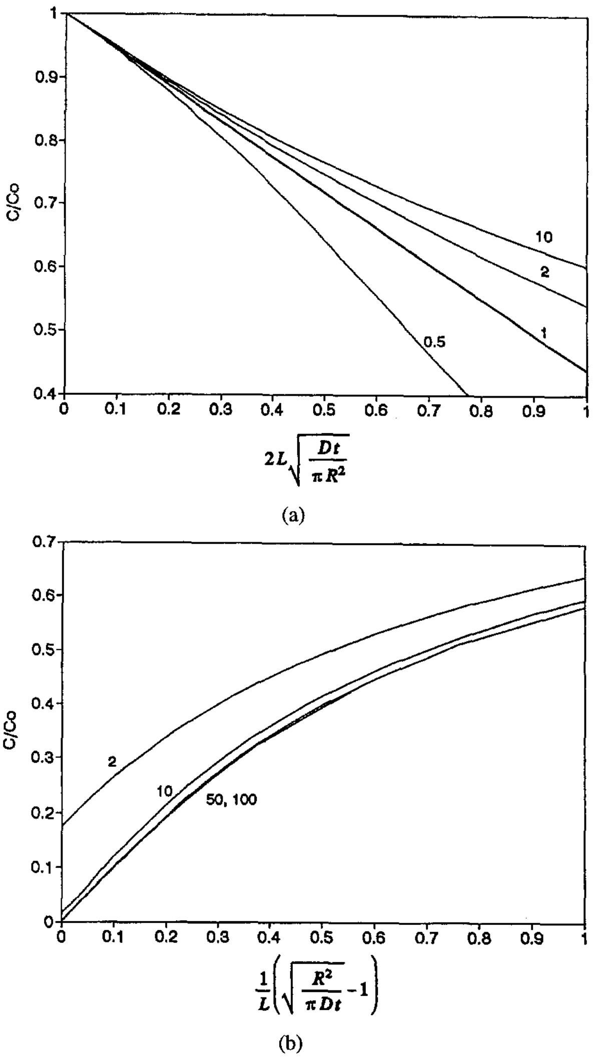

(a)

(b)

Figure 1. Theoretical desorption curves calculated from Eq. (13) (parameter L): (a) time scale: $2L\sqrt{\frac{Dt}{\pi R^2}}$ for $L \to 1$ the curves approach a linear asymptote given by Eq. (15), (b) time scale: $\frac{1}{L}(\sqrt{\frac{r^2}{\pi Dt}} - 1)$ for $L > 20$ the curves conform to Eq. (23) in the short time region.

Clearly for $L = 1$ this coincides with Eq. (15).

Comparison with the full solution (figure 1(a)) shows that this expression Eq. (18) does indeed provide a correct prediction of the short time asymptote. Equation (16) indicates that all higher terms in the series are premultiplied by ascending powers of $L - 1$, suggesting that this approximate solution will be of particular use for low values of the parameter L.

Hufton and Ruthven (1994) proposed a method of analyzing the short time region of the desorption curve based on the approximate solution of Eq. (1) for a step change in surface concentration at time (replacing Eq. (3) with $q(R) = 0$):

$$1 - \frac{\bar{q}(t)}{q_0} = \frac{6}{R}\sqrt{\frac{Dt}{\pi}} - \frac{3Dt}{R^2} \tag{19}$$

where the average concentration is given by:

$$\bar{q}(t) = \frac{3}{R^3}\int_0^R r^2 q(r,t)\,dr \tag{20}$$

Following the same logic as in the derivation of Eq. (3) using Eq. (19) to represent the desorption rate leads to the following expression for the desorption curve:

$$\frac{c}{c_0} = \frac{1}{L}\left[\sqrt{\frac{R^2}{\pi Dt}} - 1\right] \tag{21}$$

This equation cannot be correct in the limit $t \to 0$ or when L is small since under either of these conditions it predicts $c/c_0 \to \infty$, due to the assumption made on the boundary condition.

It is interesting to note that Eq. (21) can be also derived directly from the Laplace domain solution Eq. (13), considering a series expansion which is valid for large values of L:

$$\frac{\bar{c}}{c_0} = \frac{1}{s(L-1)}\left[\left(1 - \sqrt{\frac{R^2 s}{D}}\coth\left(\sqrt{\frac{s}{D}}R\right)\right) \times \sum_{n=0}^{\infty}\left(-\frac{1}{(L-1)}\sqrt{\frac{R^2 s}{D}}\coth\left(\sqrt{\frac{s}{D}}R\right)\right)^n\right] \tag{22}$$

Following the same approach as before the first order approximation is found to be

$$\frac{c}{c_0} = \frac{L-2}{(L-1)^2}\sqrt{\frac{R^2}{\pi Dt}} - \frac{1}{L-1} \approx \frac{1}{L}\left[\sqrt{\frac{R^2}{\pi Dt}} - 1\right] \tag{23}$$

We can therefore expect this approximation to be valid for large values of L, as suggested by the series expansion in Eq. (22), where all higher terms are premultiplied by ascending powers of $1/(L - 1)$.

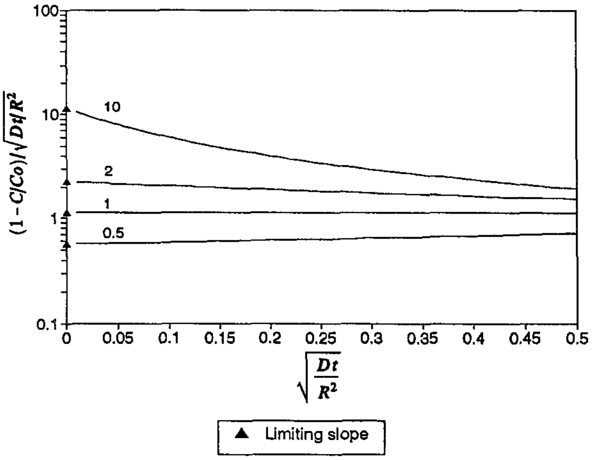

Figure 2. Plot of: $(1 - c/c_0)/\sqrt{Dt/R^2}$ vs. $\sqrt{Dt/R^2}$ showing the proposed method of extracting the time constant according to Eq. (18).

As may be seen from figure 1(b), there is a fairly wide range of conditions over which this expression does indeed provide a reasonable representation of the full solution.

The new theory Eq. (18) suggests that the appropriate plot for analysis of short time desorption data is $1 - c/c_0$ vs. $t^{1/2}$. Such a plot should pass through the origin with slope $2L(D/\pi R^2)^{1/2}$. However, from the practical point of view, the choice of time zero has a large effect on the initial slope. A more useful plot is therefore $(1 - c/c_0)/t^{1/2}$ vs. $t^{1/2}$ (figure 2). The value of $2L(D/\pi R^2)^{1/2}$ can be read directly from the intercept and the curve is almost (but not exactly) linear over a relatively large range of t. An accurate value for the zero time can then be found, once the slope is known. Repetition with different flow rates ($L\alpha F$) allows the individual values for the parameters L and D/R^2 to be derived. The validity of these values and the fit of the model to the experimental data can then be confirmed by comparing the long time portion of the curve with the theoretical curve calculated from Eq. (4) or (7) with the values of L and D/R^2 from the short time analysis.

Equilibrium Control

It is evident that, when the flow rate is sufficiently small so that the contact time is large compared with the diffusion time (R^2/D) the system should approach equilibrium. Under these conditions the desorption curve reduces to the simple exponential decay:

$$\frac{c(t)}{c_0} = \exp\left(-\frac{Ft}{KV_s}\right) \tag{24}$$

This expression may be derived directly from Eq. (4) by extracting the limit for $L \rightarrow 0$. Indeed, measurement at very low flow rates under conditions of equilibrium control was suggested by Eic and Ruthven as a useful check on the parameters derived from the higher flow rate ZLC curves. Equation (24) is a good approximation for $L < 0.5$.

Equilibration Time

The initial steps in a ZLC experiment involve equilibrating the sample with a feed stream containing a known steady concentration of sorbate. The approach to equilibrium of the effluent fluid concentration is given by Eq. (4) while approach of the adsorbed phase concentration is given by the corresponding expression given by Crank (1956):

$$\frac{\bar{q}}{q_0} = \sum_{n=1}^{\infty} \frac{6L^2 \exp\left(-\beta_n^2 \frac{Dt}{R^2}\right)}{\beta_n^2\left[\beta_n^2 + L(L-1)\right]} \tag{25}$$

From these expressions one may calculate the time required for the effluent fluid concentration and the adsorbed phase concentration to approach within 1% of their final steady values ($c/c_0 = q/q_0 = 0.99$). These curves are shown in figure 3. It is evident that the approach of the adsorbed phase to equilibrium is very much slower than that of the fluid phase concentration.

It is important to point out that the monitored variable is the concentration in the fluid phase, therefore even if the system appears to have been equilibrated this may not be true for the adsorbed phase concentration. We therefore discuss the effect of such an imbalance considering an equilibration time (i.e., Dt/R^2) that will give 99% approach to equilibrium in the fluid phase. The average adsorbed phase concentration q/q_0 at the time when $c/c_0 = 0.99$ calculated from Eq. (25) with the appropriate value for Dt/R^2 is shown as a function of L in figure 4 and the corresponding internal concentration profiles are shown in figure 5. It is clear that, especially for large L values, the internal profiles are far from uniform and the sorbate is concentrated near the external surface of the particle. It is clear that if a ZLC desorption experiment is started from this initial condition, the desorption rate will be substantially

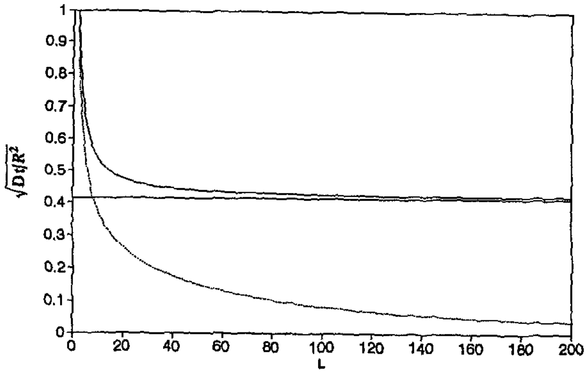

Figure 3. Time required for effluent fluid concentration (c/c_0) and adsorbed phase concentration (q/q_0) to approach within 1% of their final steady values ($c/c_0 = q/q_0 = 0.99$) calculated from Eqs. (4) and (25).

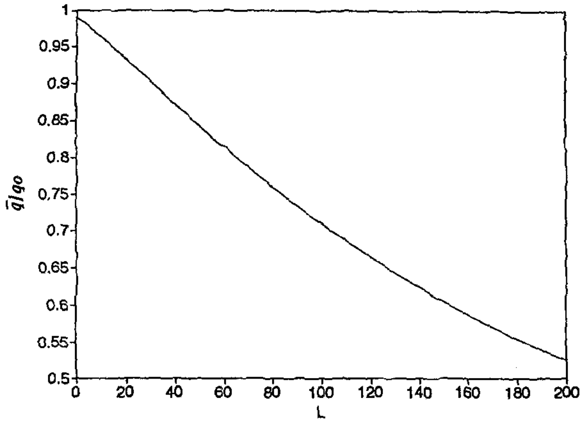

Figure 4. Variation of average adsorbed phase concentration at $c/c_0 = 0.99$ with L.

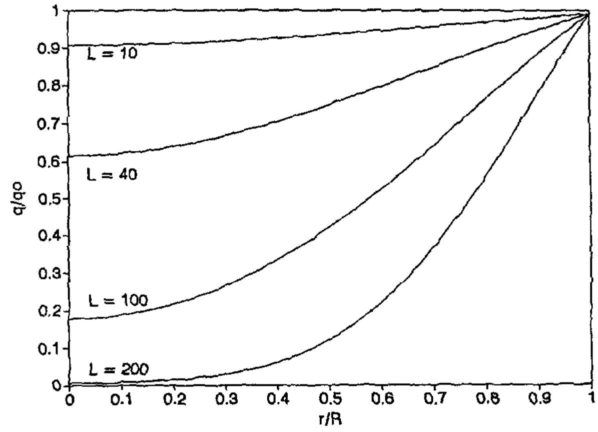

Figure 5. Concentration profile for the adsorbed phase when $c/c_0 = 0.99$.

faster than for a uniform initial distribution. Furthermore the total quantity of sorbate desorbed, as found from the overall mass balance, will be substantially smaller than the equilibrium value, leading to an erroneously low estimate of the equilibrium constant.

As may be seen from figure 3 the time required to approach equilibrium, at large L, is given approximately by 0.416 R^2/D. This asymptote can be obtained by considering the diffusion equation (Eq. (1)) with the boundary condition $q(R, t) = 0$, which gives

$$\frac{\bar{q}}{q_0} = \frac{6}{\pi^2} \sum_{n=1}^{\infty} \frac{\exp\left(-\frac{n^2\pi^2 Dt}{R^2}\right)}{n^2} \tag{26}$$

Effect of Partial Saturation on the LT Analysis

In order to discuss quantitatively the effect of partial saturation on the parameters extracted using the LT method the solution to the ZLC model subject to a square input must be derived. We consider the ZLC initially empty and we allow a time τ to charge. At time 0 the column is purged. The initial condition for the adsorbed phase Eq. (3) is therefore replaced by:

$$\frac{q(r,0)}{q_1} = 1 - \frac{R}{r} \sum_{n=1}^{\infty} \frac{2L}{\beta_n^2 + L(L-1)} \times \frac{\sin\left(\beta_n \frac{r}{R}\right)}{\sin \beta_n} \exp\left(-\beta_n^2 \frac{D}{R^2} \tau\right) \tag{27}$$

Since this affects only the initial condition, the general solution for the internal concentration profile is still:

$$q(r,t) = \sum_{n=1}^{\infty} \frac{a_n}{r} \sin\left(\beta_n \frac{r}{R}\right) \exp\left(-\beta_n^2 \frac{D}{R^2} t\right) \tag{28}$$

with β_n given by the roots of Eq. (5). Considering that the functions are orthogonal in $[0, R]$:

$$\int_0^R \sin\left(\beta_n \frac{r}{R}\right) \sin\left(\beta_m \frac{r}{R}\right) dr = 0 \tag{29}$$

the coefficients a_n can be derived in the same way as for a Fourier series. The solution is therefore given by:

$$\frac{q}{q_1} = \frac{R}{r} \sum_{n=1}^{\infty} \frac{2L}{\beta_n^2 + L(L-1)} \frac{\sin\left(\beta_n \frac{r}{R}\right)}{\sin \beta_n} \times \left[1 - \exp\left(-\beta_n^2 \frac{D}{R^2} \tau\right)\right] \exp\left(-\beta_n^2 \frac{D}{R^2} t\right) \tag{30}$$

and

$$\frac{c}{c_1} = \sum_{n=1}^{\infty} \frac{2L}{\beta_n^2 + L(L-1)} \left[1 - \exp\left(-\beta_n^2 \frac{D}{R^2} \tau\right)\right] \times \exp\left(-\beta_n^2 \frac{D}{R^2} t\right) \tag{31}$$

Considering that at time 0:

$$\frac{c_0}{c_1} = 1 - \sum_{n=1}^{\infty} \frac{2L}{\beta_n^2 + L(L-1)} \exp\left(-\beta_n^2 \frac{D}{R^2} \tau\right) \tag{32}$$

we can normalize to 1 to obtain:

$$\frac{c}{c_0} = \frac{\sum_{n=1}^{\infty} \frac{2L}{\beta_n^2 + L(L-1)} \left[1 - \exp\left(-\beta_n^2 \frac{D}{R^2} \tau\right)\right] \exp\left(-\beta_n^2 \frac{D}{R^2} t\right)}{1 - \sum_{n=1}^{\infty} \frac{2L}{\beta_n^2 + L(L-1)} \exp\left(-\beta_n^2 \frac{D}{R^2} \tau\right)} \tag{33}$$

The shape of the curve does not change, so it is difficult to detect partial saturation from a plot of the effluent concentration vs time. The LT desorption curve will be given by

$$\frac{c}{c_0} \simeq \frac{\frac{2L}{\beta_1^2 + L(L-1)} \left[1 - \exp\left(-\beta_1^2 \frac{D}{R^2} \tau\right)\right] \exp\left(-\beta_1^2 \frac{D}{R^2} t\right)}{1 - \sum_{n=1}^{\infty} \frac{2L}{\beta_n^2 + L(L-1)} \exp\left(-\beta_n^2 \frac{D}{R^2} \tau\right)} \tag{34}$$

It is evident that the largest error will be in the determination of the intercept and therefore of L. Since the intercept will be lower than the value for a uniform initial condition, the calculated value of L will be erroneously high. The effect on the value of D will be small since, at high L, β_1 is always approximately equal to π. Figure 6 shows the apparent L values calculated using Eq. (9) at 99% saturation in the fluid phase. Figure 7 shows the corresponding diffusivity values. Although the error in the equilibrium values may be large (K will be underestimated), the error in the diffusivity is less than 1%.

It should be added that in an actual experiment there may be an error in the evaluation of the baseline, as pointed out by Hufton and Ruthven (1994), therefore since all the LT analysis is carried out in a lower range of concentrations the associated error could be even larger.

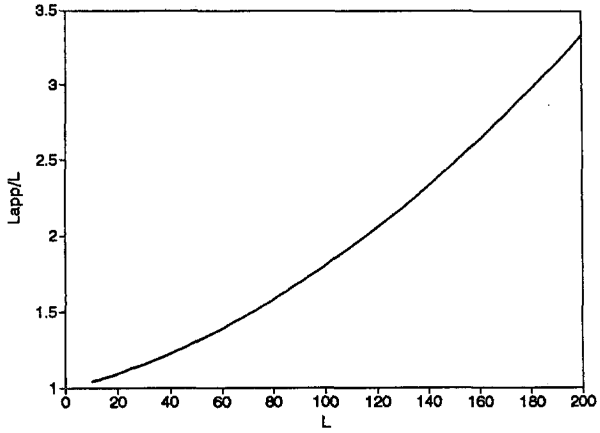

Figure 6. Error in the value of L calculated from the intercept of the plot of $\ln(c/c_o$ vs. $t)$ when the initial condition is at $c/c_0 = 0.99$ rather than true equilibrium).

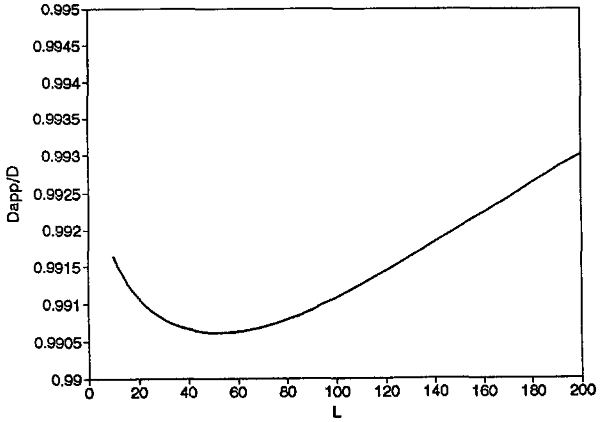

Figure 7. Error in diffusivity value calculated for the LT analysis of the ZLC desorption curve when the initial condition is $c/c_0 = 0.99$ (rather than true equilibrium).

Effect of Partial Saturation on the ST Analysis

To derive an approximation valid for short times the ZLC model must be solved by Laplace transformation. Considering the change of variables $\xi = rq$, in the Laplace domain we have:

$$D\frac{d^2\tilde{\xi}}{dr^2} = s\tilde{\xi} - rq_1 - Rq_1\sum_{n=1}^{\infty}\frac{2L}{\beta_n^2 + L(L-1)} \times \frac{\sin\left(\beta_n\frac{R}{r}\right)}{\sin\beta_n}\exp\left(-\beta_n^2\frac{D}{R^2}\tau\right) \qquad (35)$$

which has as a general solution:

$$\tilde{\xi} = a_1\exp\sqrt{\frac{sr^2}{D}} + a_2\exp -\sqrt{\frac{sr^2}{D}} + \frac{rq_1}{s} - Rq_1 \times \sum_{n=1}^{\infty}\frac{2L}{\beta_n^2 + L(L-1)}\frac{\sin\left(\beta_n\frac{r}{R}\right)}{\sin\beta_n}\frac{\exp\left(-\beta_n^2\frac{D}{R^2}\tau\right)}{s + \beta_n^2\frac{D}{R^2}} \qquad (36)$$

We are interested in the approximation for high L. Applying the same constraints as those used in deriving Eq. (19) (Crank, 1956)

$$\frac{\bar{q}(s)}{q_1} = \left(\sum_{n=1}^{\infty}\frac{6L}{\beta_n^2 + L(L-1)}\frac{\exp\left(-\beta_n^2\frac{D}{R^2}\tau\right)}{s + \beta_n^2\frac{D}{R^2}} - \frac{3}{s}\right) \times \left(\sqrt{\frac{D}{sR^2}}\coth\sqrt{\frac{sR^2}{D}} - \frac{D}{sR^2}\right) + \frac{1}{s} - \sum_{n=1}^{\infty}\frac{6L^2}{\beta_n^2\left[\beta_n^2 + L(L-1)\right]}\frac{\exp\left(-\beta_n^2\frac{D}{R^2}\tau\right)}{s + \beta_n^2\frac{D}{R^2}} \qquad (37)$$

Inverting this solution using tables of Laplace transforms (Roberts and Kaufman, 1966) and considering only the relevant terms in the short time, the following approximation is found for high values of L:

$$\frac{c}{c_o} \simeq \frac{1}{L}\left[\sqrt{\frac{R^2}{\pi Dt}} - \frac{1 + (L-1)\sum_{n=1}^{\infty}\frac{2L}{\beta_n^2 + L(L-1)}\exp\left(-\beta_n^2\frac{D}{R^2}\tau\right)}{1 - \sum_{n=1}^{\infty}\frac{2L}{\beta_n^2 + L(L-1)}\exp\left(-\beta_n^2\frac{D}{R^2}\tau\right)}\right] \qquad (38)$$

It is evident that, again, the slope of the desorption curve is unchanged so it is difficult to detect partial saturation simply from the form of the ZLC response curve. The slope remains the same but again the intercept is affected. The deviation is proportional to $1/L$ and the apparent L is lower as can be seen from figure 8. Since the derived diffusivity is proportional to $1/L^2$ the apparent D can be overestimated by as much as an order of magnitude, as shown in figure 9. The error in the K values will therefore be proportional to L, and the apparent K will be larger.

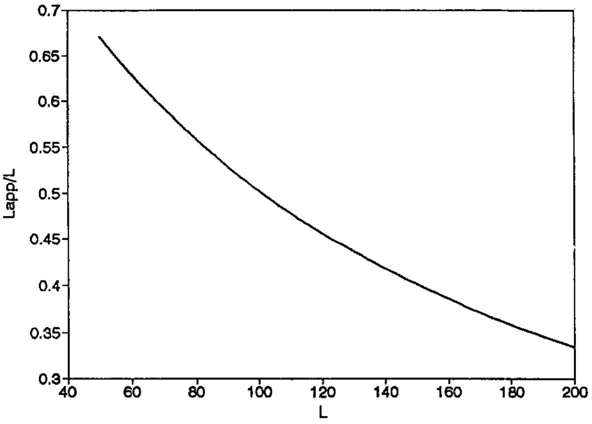

Figure 8. Error in value of L calculated from the short time analysis when the initial condition is $c/c_0 = 0.99$ rather than true equilibrium.

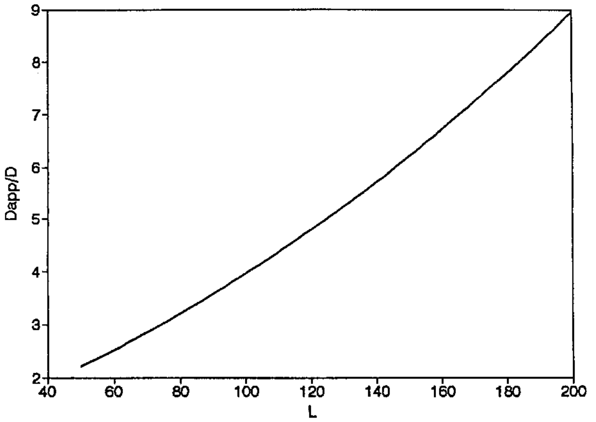

Figure 9. Error in value of D calculated from the short time analysis. When the initial condition is $c/c_0 = 0.99$ rather than true equilibrium.

Table 1. Experimental conditions and parameter values for propane-NaX at 85°C.

	Figure 11(a)	Figure 11(b)
T, °C	85	85
Type of experiment	Tracer ZLC	Normal ZLC
P_{propane}, Torr	760	~0
F, cc/min	11.8	14.2
D/R^2 (s^{-1})	8.4×10^{-3}	4.8×10^{-3}
L	158	63
τ, s	6.5	5.2
R (μm)	50	50

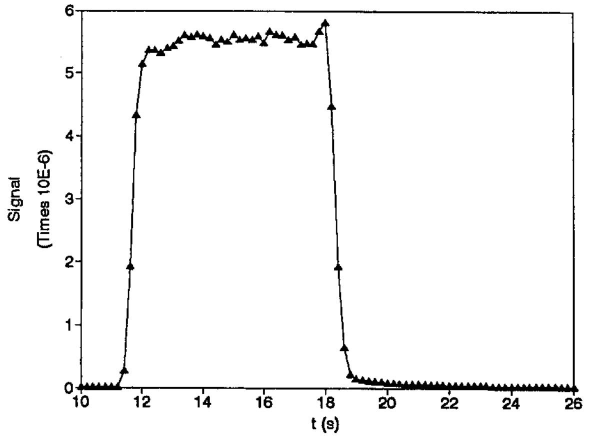

Figure 10. Effluent concentration history during partial saturation and desorption of NaX zeolite with propane at 85°C.

Partial Saturation—Experimental Study

In order to illustrate the effects of incomplete equilibration on the ZLC desorption curve we carried out a brief experimental study for the system C_3H_8-NaX zeolite (100 μm crystals). The experimental conditions together with relevant parameters are summarized in Table 1.

Prior to the experiments the ZLC sample was regenerated at 300°C overnight in a helium purge. In the initial series of experiments a period of 15–20 minutes was allowed for the equilibration process. The ZLC desorption curves and the derived parameters were shown to be reproducible and insensitive to the equilibration time, showing that true equilibrium was indeed reached. The values of L and D/R^2 given in Table 1 were derived from these experiments.

In a second series of experiments the sample was equilibrated for only a few seconds before purging at the same flowrate as in the earlier experiments. A typical experimental adsorption and desorption curve is shown in figure 10. From this plot the value of the equilibration time can be accurately measured. Figure 11 shows experimental desorption curves together with the curves for the well equilibrated samples (under the same conditions) and the theoretical curves for partial saturation predicted according to Eq. (33) using the parameters D/R^2 and L derived from the true curves (for the fully equilibrated sample) and the measured equilibration time. It is clear that the theory provides an excellent prediction of the observed behaviour thus confirming the validity of the analysis.

A straightforward extension of this approach would seem to provide a simple and convenient way of

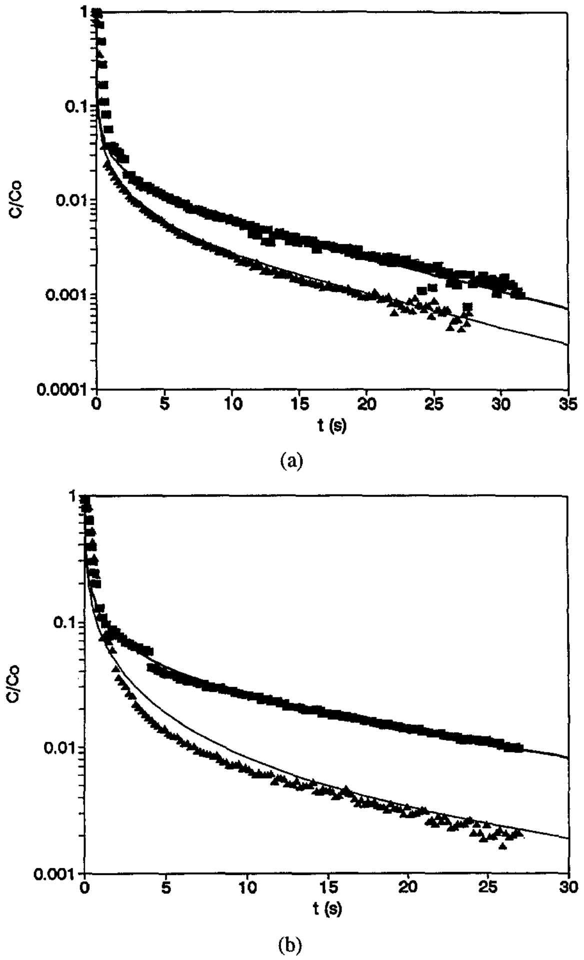

Figure 11. Experimental ZLC desorption curves for propane—NaX at 85°C for a fully equilibrated sample (■) and a partially equilibrated sample (▲). Theoretical curves for the partially saturated cases are calculated according to Eq. (33) with the parameters (D/R^2 and L). For details see Table 1.

establishing the dominance of intracrystalline diffusion in a ZLC experiment. If the desorption rate were controlled by a surface barrier resistance, rather than by intracrystalline diffusion, the profile of adsorbed phase concentration through the crystal would be uniform at all times, even under conditions of partial saturation. The resulting expressions for the ZLC controlled by a surface barrier, subject to a square input, are given by (details of the derivation can be found in the Appendix):

$$\frac{c}{c_0} = \frac{1 - \exp\left(-\frac{L'}{L'+1}k\tau\right)2}{1 - \frac{1}{L'+1}\exp\left(-\frac{L'}{L'+1}k\tau\right)} \frac{\exp\left(-\frac{L'}{L'+1}kt\right)}{L'+1} \tag{39}$$

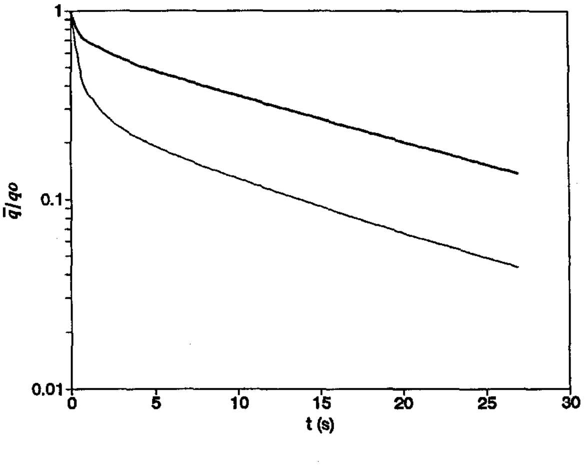

Figure 12. Time dependence of average adsorbed phase concentration calculated by integration of the desorption curves of figure 11(b).

and:

$$\frac{\bar{q}}{q_0} = \exp\left(-\frac{L'}{L'+1}kt\right) \tag{40}$$

Equation (39) has the same general form as Eq. (34). The measurable variable c/c_0 therefore cannot be used to provide a direct indication of the controlling mass transfer resistance.

Considering that:

$$1 - \frac{\bar{q}}{q_0} = \frac{\int_0^t \frac{c}{c_0}\,dt}{\int_0^\infty \frac{c}{c_0}\,dt} \tag{41}$$

it is however possible to identify indirectly the controlling process since in the case of a surface barrier the dimensionless ZLC desorption curve for the adsorbed phase concentration will remain the same for full and partial saturation initial conditions. Figure 12 shows the total adsorbed phase concentration calculated by integration of the experimental desorption curves shown in figure 11(b). The present results show clearly that there is a significant difference between these curves and this may be taken as *prima facie* evidence that under the experimental conditions the desorption rate is indeed controlled by intracrystalline diffusion. The large deviation from the reported NMR self-diffusivity for the system C_3H_8-NaX (Pfeifer et al., 1966) ($D \sim 10^{-4}$ cm^2 s^{-1} compared with $\sim 10^{-7}$ cm^2 s^{-1}), which is entirely consistent with the behaviour reported by Eic and Ruthven for higher hydrocarbons in NaX (Eic and Ruthven, 1988), therefore cannot be attributed to the intrusion of a surface barrier resistance.

Conclusions

In order to properly apply the proposed methods it is necessary to allow the system to reach full equilibrium; therefore the charging time for high L values should be at least 0.5 R^2/D. When the L value is large (>10) the interpretation of an experimental ZLC desorption curve is unambiguous and the original method of analysis based on an experimental decay of the concentration in the long time region yields reliable values for the diffusional time constant (and the equilibrium). Analysis in accordance with Eq. (21) (the intermediate time approximation) provides an acceptable alternative for $L > 20$. However, for rapidly diffusing and strongly adsorbed species it is not always possible in practice to achieve experimental conditions corresponding to a high L value, so it is important to understand the extent to which reliable diffusivity values can be derived from desorption curves at low or intermediate L values. For $0.5 < L < 5.0$ the traditional analysis yields unreliable parameter values but the short time analysis based on Eq. (18)—a plot of:

$$(1 - c/c_0)/\sqrt{t} \text{ vs. } \sqrt{t}$$

can still yield a reliable estimate of the time constant, provided that the measurements are carried out over a range of flow rates.

For $L < 0.5$ the system is essentially equilibrium controlled (Eq. (24)) and no reliable kinetic data can be extracted from the desorption curve. Under these conditions the plot of:

$$(1 - c/c_0)/\sqrt{t} \text{ vs. } \sqrt{t}$$

has a strong positive slope so the conditions of equilibrium control are easily diagnosed.

There is a considerable range ($L > 5$) over which both the short time and long time analysis are feasible. Under these conditions consistency of the model parameters from the ST and LT analyses can be checked to confirm the validity of the theoretical model (see for example Cavalcante (1994)).

It has been shown that the partial saturation experiment can be used to discriminate between surface barrier and intracrystalline diffusion processes.

Notation

a_n	coefficients in Eq. (36)	
c	fluid phase concentration of sorbate	mol/m^3
c_0	initial steady value of c	mol/m^3
D	diffusivity	m^2/s
F	purge flow rate	m^3/s
K	equilibrium ratio (q^*/c)	—
L	defined by Eq. (6)	—
L'	defined by Eq. (A7)	—
q	adsorbed phase concentration	mol/m^3
q^*	value of q at equilibrium with gas phase concentration c	mol/m^3
$\bar{q}$	average value of q over zeolite crystal	mol/m^3
q_0	value of q at equilibrium with c_0	mol/m^3
r	radial coordinate	m
R	crystal radius	m
s	transform variable	s^{-1}
t	time	s
V_f	fluid volume in ZLC cell	m^3
V_s	solid volume in ZLC cell	m^3
α	$V_f/3KV_s$	—
α'	V_f/KV_s	—
ξ	rq	mol/m^2

Appendix

The set of equations used to describe a ZLC controlled by a surface barrier are (Ruthven and Stapleton, 1993):

$$V_s\frac{dq}{dt} + V_f\frac{dc}{dt} + F(c - c_1) = 0 \tag{A1}$$

$$\frac{dq}{dt} = k(Kc - q); \qquad q = \bar{q} \tag{A2}$$

We are interested in the solution for a square wave input. For the initial adsorption step the Laplace transforms of Eqs. (A1) and (A2) are:

$$V_s s\tilde{q} + V_f s\tilde{c} + F\left(\tilde{c} - \frac{c_1}{s}\right) = 0 \tag{A3}$$

$$s\tilde{q} = k(K\tilde{c} - \tilde{q}) \tag{A4}$$

which can be solved to give:

$$\frac{\tilde{c}}{c_1} = \frac{1}{s}\frac{F(s+k)}{sV_f(s+k) + skKV_s + F(s+k)} \tag{A5}$$

$$\tilde{q} = \frac{kK\tilde{c}}{s+k} \tag{A6}$$

and defining:

$$L' = \frac{F}{kKV_s}; \qquad \gamma' = \frac{V_f}{KV_s} \tag{A7}$$

the following solution can be obtained in the time domain either through direct inversion (Ruthven and Stapleton, 1993) or through the method of residues:

$$\frac{c}{c_1} = 1 - \sum_{i=1}^{2} \frac{1 + \gamma' - \alpha_i \gamma'}{L' + \gamma' + 1 - 2\alpha_i \gamma'} \exp(-\alpha_i k t) \tag{A8}$$

$$\frac{q}{q_1} = 1 - \sum_{i=1}^{2} \frac{L' + \gamma' + 1 - \alpha_i \gamma'}{L' + \gamma' + 1 - 2\alpha_i \gamma'} \exp(-\alpha_i k t) \tag{A9}$$

with

$$\alpha_{1,2} = \frac{L' + \gamma' + 1 \pm \sqrt{(L' + \gamma' + 1)^2 - 4\gamma' L'}}{2\gamma'} \tag{A10}$$

For the desorption step the Laplace Transforms of Eqs. (A1) and (A2) are:

$$V_s(s\tilde{q} - q_0) + V_f(s\tilde{c} - c_0) + F\tilde{c} = 0 \tag{A11}$$

$$s\tilde{q} - q_0 = k(K\tilde{c} - \tilde{q}) \tag{A12}$$

Following the same procedure as above the following solutions are found:

$$\frac{c}{c_0} = \sum_{i=1}^{2} \frac{\frac{q_0}{Kc_0} + \gamma' - \alpha_i \gamma'}{L' + \gamma' + 1 - 2\alpha_i \gamma'} \exp(-\alpha_i k t) \tag{A13}$$

$$\frac{q}{q_0} = \sum_{i=1}^{2} \frac{L' + \gamma' \frac{Kc_0}{q_0} + 1 - \alpha_i \gamma'}{L' + \gamma' + 1 - 2\alpha_i \gamma'} \exp(-\alpha_i k t) \tag{A14}$$

which in the limit as $\gamma' \rightarrow 0$ reduce to Eqs. (39) and (40).

Acknowledgment

Partial financial support provided by the Petroleum Research Fund is gratefully acknowledged.

References

Eic, M. and D.M. Ruthven, *Zeolities*, **8**, 40 (1988).

Ruthven, D.M. and M. Eic, *Am. Chem. Soc. Symp, Series*, **368**, 362–375 *Perspectives in Molecular Sieve Science Ch. 22*, W.H. Flank and T.E. Whyte (Eds.) Am. Chem. Soc., Washington D.C. (1988).

Voogd, P., H. van Bekkum, D. Shavit, and H.W. Kouwenhovem, *J. Chem. Soc. Faraday Trans.* I, **87**, 3575 (1991).

Ruthven, D.M. and Z. Xu, *Chem. Eng. Sci.*, **48**, 3307 (1993).

Ruthven, D.M. and P. Stapleton, *Chem. Eng. Sci.*, **48**, 89 (1993).

Hufton, J.R. and D.M. Ruthven, *Ind. Eng. Chem. Research*, **32**, 2379 (1993).

Micke, A., M. Kocirik, and M. Bulow, *Ber. Bunsenges. Phys. Chem.*, **98**, 242 (1994).

Hufton, J.R., S. Brandani, and D.M., Ruthven, *10th International Zeolite Conference*, Garmish (1994).

Crank, J., *The Mathematics of Diffusion*, Oxford University Press, London, 1956.

Brandani, S. and D.M. Ruthven, *Chem. Eng. Sci.*, **50**, 2055 (1995).

Roberts, G.E. and H. Kaufman, *Tables of Laplace Transforms*, Saunders, Philadelphia, 1966.

Pfeifer, H., J. Karger, A. Germanus, W. Schirmer, M. Bulow, and J. Caro, *Adsorption Science and Technology*, **2**, 229 (1985).

Eic, M. and D.M. Ruthven, *Zeolities*, **8**, 472 (1988)

Cavalcante, C., Ph.D. thesis, University of New Brunswick, Fredericton (1994).